Host–guest and guest–guest interactions between xylene isomers confined in the MIL-47(V) pore system

An Ghysels · Matthias Vandichel · Toon Verstraelen ·
Monique A. van der Veen · Dirk E. De Vos ·
Michel Waroquier · Veronique Van Speybroeck

Abstract The porous MIL-47 material shows a selective adsorption behavior for para-, ortho-, and meta-isomers of xylenes, making the material a serious candidate for separation applications. The origin of the selectivity lies in the differences in interactions (energetic) and confining (entropic). This paper investigates the xylene–framework interactions and the xylene–xylene interactions with quantum mechanical calculations, using a dispersion-corrected density functional and periodic boundary conditions to describe the crystal. First, the strength and geometrical characteristics of the optimal xylene–xylene interactions are quantified by studying the pure and mixed pairs in gas phase. An extended set of initial structures is created and optimized to sample as many relative orientations and distances as possible. Next, the pairs are brought in the pores of MIL-47. The interaction with the terephthalic linkers and other xylenes increases the stacking energy in gas phase (−31.7 kJ/mol per pair) by roughly a factor four in the fully loaded state (−58.3 kJ/mol per xylene). Our decomposition of the adsorption energy shows various trends in the contributing xylene–xylene interactions. The absence of a significant difference in energetics between the isomers indicates that entropic effects must be mainly responsible for the separation behavior.

Keywords Adsorption · MIL-47 · DFT-D · Xylenes · Separation

1 Introduction

Since a couple of years, metal organic frameworks (MOFs) are a topical theme; they represent a new class of porous materials with extraordinary physicochemical and mechanical properties due to their hybrid architecture of organic and inorganic building blocks [1–3]. Their applications in the field of gas adsorption, storage, gas separation, and catalysis are almost inexhaustible due to the specificity of the hybrid organic–inorganic composition [4–7]. Examples of their fascinating properties are the flexibility of the framework, the appearance of catalytic sites in the pores, etc. These are a consequence of the unique combination of properties typical for metals and organic species.

In previous work, some of the authors showed that metal organic frameworks could be successfully used as selective adsorbents for the industrially relevant separations of para-xylene (pX) versus meta-xylene (mX) and ortho-xylene (oX) versus ethylbenzene (eB) [8–10]. The separation of mixed C8 alkylaromatic compounds is one of the most challenging issues in the chemical industry, for example because of its direct link with PET production [11]. Among the various types of MOFs that have been tested, the MIL-47 material proved to be very successful. This MOF

A. Ghysels (✉) · M. Vandichel · T. Verstraelen ·
M. Waroquier · V. Van Speybroeck (✉)
Center for Molecular Modeling, Quantum Chemistry-Molecular
Modeling Alliance, Ghent University, Technologiepark 903,
9052 Ghent, Belgium
e-mail: an.ghysels@ugent.be

V. Van Speybroeck
e-mail: veronique.vanspeybroeck@ugent.be

M. A. van der Veen · D. E. De Vos
Centre for Surface Chemistry and Catalysis, KU Leuven,
Kasteelpark Arenberg 23, 3001 Heverlee, Belgium
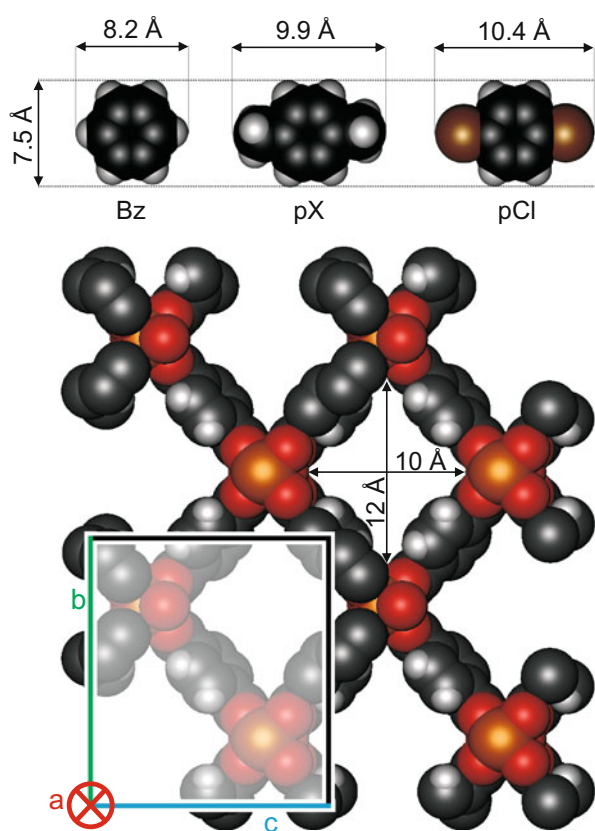
Fig. 1 MIL-47 consists of terephthalic linkers connected by VO^{2+} ions. Xylenes adsorb well in the one-dimensional pore channels. View along the a direction; four unit cells are displayed. The pore dimensions of MIL-47 and the characteristic dimensions of the adsorbates are estimated by assigning van der Waals radii to the atoms

consists of one-dimensional pores in which terephthalate ligands are connected by VO^{2+} ions (Fig. 1). MIL-47 is one of an impressive series of MOFs that were synthesized by Férey et al. [12]. It is not completely clear what mechanism is responsible for the preference of adsorption between the three types of xylene isomers and ethylbenzene. In this paper, we try to unravel the molecular interactions between pairs of adsorbed xylenes and between xylenes and organic linkers using in silico experiments. The interactions are studied with quantum mechanical periodic modeling. Once the mechanism of selectivity in adsorption has been understood, the obtained knowledge can be used for designing new materials with tailor-made properties toward gas separation and to possibly modify the organic linkers to control the affinity for specific aromatic adsorbates.

Long-range dispersion interactions and more particularly π–π stacking interactions will manifestly play an important role for the organization of xylenes in the pore. Basically, only very advanced ab initio correlated wave function methods are able to account for these effects, but

they are computationally too demanding to apply to our system. Nowadays, density functional theory (DFT) is the most widely used method for electronic structure calculations for extended molecular systems, but without modifications, these methods are not able to account for long-range electrostatic correlations that are responsible for the dispersion forces. Grimme et al. [13–15] proposed the DFT-D method in which an empirical $C_6 R^{-6}$ correction is added to the standard density functionals. This method is able to account for the π–π interactions in MOFs [14].

Several molecular modeling studies investigated various adsorbates with grand canonical Monte Carlo techniques (GCMC) on MIL-47: N_2 [16], CO_2 [17], CH_4 [18], H_2 [19], and xylenes [20]. GCMC techniques usually rely on fast classical force field descriptions of the global potential energy of the system. So, GCMC techniques allow a fast computation of thermodynamic quantities and they have been frequently and successfully applied to explain separations over MOFs [16, 20–24]. The force fields required to perform the molecular simulations are taken from the literature. The accuracy of these classical approaches will certainly be improved in the near future when more advanced force fields are available for these particular MOFs that also account for the flexibility of the framework [25]. In the MIL-47 study by Castillo et al. [20], good agreement is found with isotherm experiments using a model with partial atomic charges and the Lennard-Jones potential for the van der Waals interactions. The framework is kept rigid during the simulations. The computed mixture isotherms of the xylene isomers lead to separation factors in MIL-47 predicting a preferential adsorption for ortho-xylene (oX), closely followed by para (pX), and then meta (mX). The adsorption selectivity was found to increase with pressure and the results agree with the experimental findings. The computed adsorption isotherms manifestly overestimate the loading of para- and ortho-xylene at the lowest temperatures. The authors attribute this discrepancy to small changes in the framework structure with temperature. The saturation loading reached in their simulations was about 4 molecules per unit cell, while experimentally the maximum loading was 3.4 molecules per unit cell [8, 9].

The selectivity of xylene isomers in MIL-47 most likely originates from packing effects, as suggested by Alaerts and Finsy et al. [8, 9]. It has been speculated that molecules are adsorbed by pairs at high loadings, their benzene rings facing each other and approximately parallel to the aromatic rings of the terephthalate linkers. Additionally, the spatial arrangement of the methyl groups of each xylene should play a significant role in the determination of the preferential adsorption. It is suspected that the crude force field used in the work of Castillo et al. cannot properly describe these packing effects. With the current lack of

suitable more accurate force fields, quantum chemical DFT-D calculations can give some added value in the underlying mechanism for the selective adsorption of xylene isomers. Stacking effects are more accurately described when taking into account the long-range dispersion interactions by using the empirical Grimme corrections [13] complementary to the standard density functionals. A DFT-D approach also has the advantage that the adsorption and stacking energy can be decoupled in various contributions elucidating the interactions responsible for the observed different adsorption behavior. In contrast to the molecular simulations of Castillo et al. [20], we also incorporate in this study the packing of mixed xylene pairs such as pX–oX, pX–mX and oX–mX.

In this work, we first investigate xylene–xylene interactions in the gas phase. The strength of the xylene stacking energy is compared to the stacking energy of benzene pairs and dichlorobenzene pairs. Benzene stacking is well studied [26–28], and dichlorobenzene adsorption shows experimentally a similar selectivity behavior in MIL-47 as xylenes [29]. Next, the pairs are embedded in the MIL-47 framework respecting the maximum loading of two xylene pairs in one unit cell. An extensive set of configurations for the adsorbed xylenes is generated. As such, we are able to validate the effect of the confined environment and interaction with the walls of the material. The adsorption energy of the most stable configuration is studied in detail using an energy decomposition scheme to achieve more insight into the host–guest and guest–guest interactions.

2 Computational methods

2.1 Characterization of a xylene pair

A thorough study on the interaction between xylene pairs will be performed, and thus it is essential to give a good definition of their relative position with respect to each other. The relative position and orientation of a xylene pair is characterized by attaching a Cartesian coordinate frame to each xylene (Fig. 2a) [30] denoted as (O_1, x_1, y_1, z_1) and (O_2, x_2, y_2, z_2) for the two xylenes, X_1 and X_2, respectively. The x-axis always coincides with the twofold rotational symmetry axis of each xylene. Note that in the three-dimensional structure, the orientation of the methyl groups may prevent the existence of this C_2 symmetry, but the symmetry axis is always present in the projection on paper (Fig. 2a). The sense of z_2 is chosen such that the angle between z_1 and z_2 is less than 90°. In principle, the relative orientation of two molecules is completely characterized by six parameters. For this work, we only consider the four most important internal coordinate parameters to describe
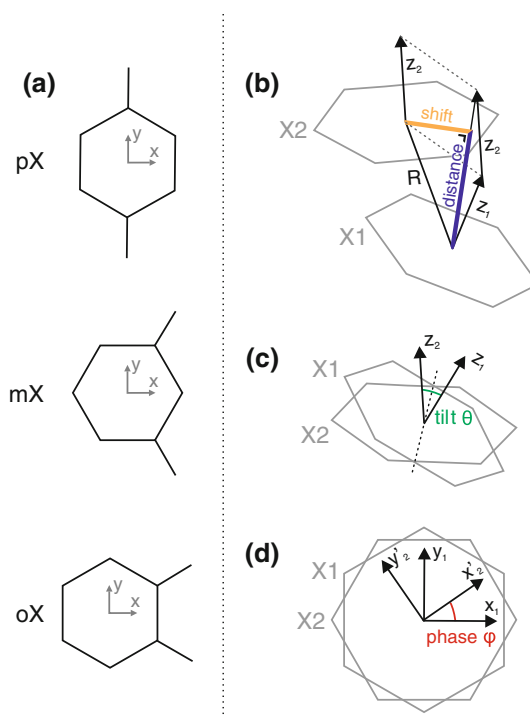
Fig. 2 A coordinate system is attached to each xylene (X_1 and X_2) in a xylene pair. Four parameters are defined to describe their relative position and orientation: shift (s), distance (d), tilt (θ), and phase (φ)

their relative orientation: distance (d), shift (s), tilt (θ), and phase (φ). These are defined below such that an interchange of X_1 and X_2 or a point inversion results in the same values for these four parameters.

The distance parameter d is the length of the projection of the vector $\boldsymbol{R}$ (connecting the centers of the six-membered rings) on the vector $z_1 + z_2$ (Fig. 2b). The length of the orthogonal complement in this projection is called the shift s. Next, X_2 is translated over the vector $\boldsymbol{R}$ to bring the geometric centers of the six-membered rings on top of each other (Fig. 2c). The tilt θ is defined as the angle between the z_1- and z_2-axis. X_2 is then rotated over θ about the vector $z_1 \times z_2$, such that $(O_2', x_2, y_2, z_2) \rightarrow (O_2', x_2', y_2', z_1)$; the z-axes of the xylenes are now aligned and the x-axes and y-axes lie in the same plane (Fig. 2d). Finally, the phase φ is determined as the absolute value of the angle between the x_1- and x_2'-axis.

The above procedure is also applied to a benzene pair and dichlorobenzene pairs.

2.2 Quantumchemical modeling

Density functional theory calculations are carried out using the CPMD code, which allows to simulate systems with periodic boundary conditions [31]. The BP exchange correlation functional [32] is used with ultrasoft Vanderbilt pseudopotentials [33], especially designed to work with a

25 Ry cut off for the auxiliary plane wave grid. To include the possible effects of π–π interactions, the BP functional is combined with the Grimme dispersion correction for van der Waals interactions [13]. Three types of systems are simulated: xylenes in vacuum, the empty MIL-47 framework, and the fully loaded MIL-47 framework with four xylenes per unit cell.

Vacuum calculations of a xylene molecule or a pair of xylenes are performed in a large box of $20 \times 20 \times 20$ Å^3 and are labeled with 'vac'. The investigated molecules are para-xylene (pX), ortho-xylene (oX), and meta-xylene (mX). In addition, benzene (Bz) and dichlorobenzenes in para-, ortho-, and meta-configuration (pCl, oCl, mCl) are simulated in vacuum for comparison.

The initial framework geometry of the empty MIL-47 is taken directly from the refined structure obtained by X-ray diffraction (Supp. Info. of Ref. [12], CCDC-166785, orthorhombic unit cell with $a = 6.8179$ Å, $b = 16.1433$ Å, $c = 13.9392$ Å). In the energy minimization, the internal coordinates are optimized while the unit cell parameters are kept fixed at the experimental values. The metal V^{4+} ions in MIL-47 have each spin ½. The unit cell containing four vanadium centers can have a total spin of 0, 1, or 2. The most stable structure corresponds with $S = 1$, and the gain in energy with respect to the $S = 0$ system amounts to 80 kJ/mol per unit cell. As adsorption energies require the computation of differences in energy, the differences due to the usage of another spin state cancel out if we consistently use the same total spin for the framework. In view of the computational cost, all calculations were performed with $S = 0$.

In the fully loaded state, two xylene pairs are inserted in the pores of MIL-47 with the Zeobuilder package [34], and the geometry is optimized with CPMD [31]. The experimental unit cell parameters are used when MIL-47 is fully loaded with pure pX, oX, or mX (codes CCDC-632101, CCDC-632102, CCDC-632103, respectively [8]). Because of lack of experimental values during multicomponent adsorption experiments, the cell parameters are chosen somewhat arbitrarily when MIL-47 is fully loaded with a mixture of the xylene isomers: the pure oX experimental parameters for the pX–oX mixture (code CCDC-632102 [8]) and the empty framework parameters for pX–mX and oX–mX mixtures (code CCDC-166785 [12]). The variation in cell parameters among the structures is minimal, and keeping them fixed during the geometry optimization is an approximation whose effect is expected to largely cancel when calculating energy differences. The coordinate files of the optimized structures are available in the Supporting Information for the empty framework and the various fully loaded states. The decomposition of adsorption energies in Sect. 3 is derived from static calculations, where xylenes or framework atoms are removed from the fully loaded state

and the energy is calculated without prior geometry optimization. These energies are labeled with 'stat'.

3 Results and discussion

3.1 Guest–guest interactions in gas phase

Before tackling the xylenes interactions in the MIL-47 pore system, it is useful to have an understanding of the stacking of xylenes in the gas phase. Therefore, we construct a series of xylene pairs, and the geometry and the stacking energy are investigated for each of them. The geometry is characterized by the four geometry parameters in Fig. 2: shift, distance, tilt, and phase. The stacking energy is calculated from the optimized geometry of the individual xylene molecules X_1 and X_2 and of a xylene pair P_{12}. The *stacking energy* is defined as

$$\Delta E_{\text{stack}}^{\text{vac}}(P_{12}) = E^{\text{vac}}(P_{12}) - E^{\text{vac}}(X_1) - E^{\text{vac}}(X_2) \qquad (1)$$

Six pairs are studied: 'pure' pairs (pX–pX, oX–oX, mX–mX) and 'mixed' pairs (oX–mX, oX–pX, pX–mX). An extensive set of initial structures (Fig. 3) is generated by varying the distance d and the phase φ between the pairs: d varies between 2.8 and 4.6 Å with steps of 0.2 Å, while φ is increased with steps of 30° until a symmetrically equivalent structure is met. The initial shift s and tilt θ are set to zero. The geometries of these 330 initial structures are optimized in a large box (vacuum). For each pair, the optimized geometries are ordered according to increasing energy ($E_1, E_2,\ldots$).

Table 1 presents the geometrical properties and stacking energies for the following two cases. First, the geometrical properties are calculated for the geometry with the lowest energy E_1. Second, in case of thermal equilibrium, the thermal average of a property A is obtained by weighting the contribution of each geometry by its Boltzmann probability $p(E_i)$,

$$p(E_i) = \exp\left(-\frac{E_i}{k_B T}\right) \bigg/ \sum_j \exp\left(-\frac{E_j}{k_B T}\right) \qquad (2)$$

$$\langle A \rangle = \sum_i p(E_i)A(i) \qquad (3)$$

with T the temperature and k_B the Boltzmann constant. Due to temperature, not only the lowest energy state E_1 of a pair is populated, but also nearby minima can be reached. It should be noted, however, that our formula only sums over local minima but no nearby non-equilibrium states, which would be required for accurate thermodynamics.

The probability distribution $p(E_i)$ favors the lowest energy geometry E_1 largely at 300 K (highly peaked distribution in Supp. Info. Fig. 1), making this geometry the
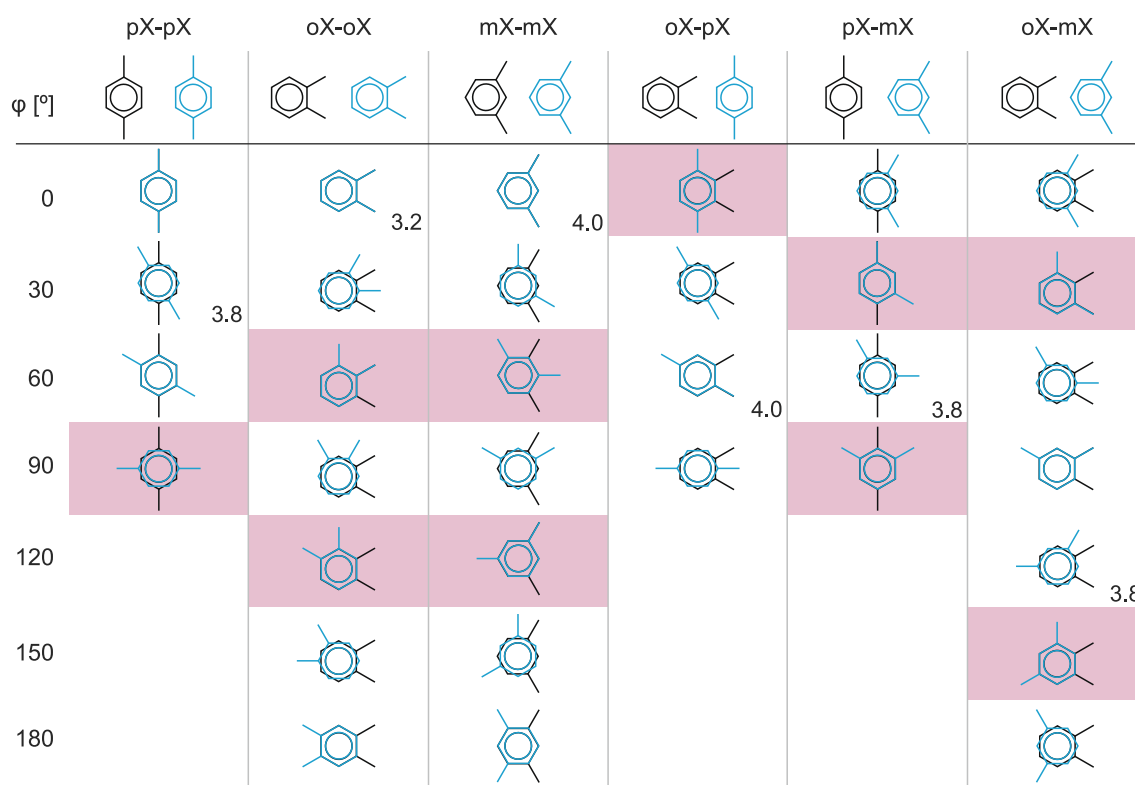
Fig. 3 Initial geometries of six xylene pairs are obtained by varying the phase φ and the distance d. A similar study is performed for dichlorobenzene pairs. Orientations that do not fit in the MIL-47 pores are given a *red* background. The initial geometries leading to the most stable structure are labeled with the initial distance

dominant contribution to the sum in Eq. (3). Indeed, the lowest energy properties correlate well with the thermal average properties in Table 1. Figure 4 illustrates the shift and distance parameters in the optimized benzene pair and the most stable pure xylene pairs. Clearly, the pairs take the parallel-displaced configuration.

The stacking energy $\Delta E_{\text{stack}}^{\text{vac}}$ is favorable for benzene, xylenes, and dichlorobenzenes. Xylene pairs are the most stable with an average stacking energy of -31.7 kJ/mol, followed by the dichlorobenzene pairs with -24.3 kJ/mol and benzene pairs with -19.7 kJ/mol. Aromatic π–π stacking has been extensively studied for benzene pairs [35–43], and it was found that T-shaped and parallel-displaced configurations have nearly equal stacking energy, being slightly more stable than the face-to-face sandwich configuration [26–28]. The benzene pair geometry in Table 1 is the parallel-displaced configuration. These studies also indicate that substituents typically make the stacking stronger with respect to benzene stacking, which is confirmed in our results for methyl and chlorine substituents [44–46].

Moreover, Table 1 suggests a relationship between the stacking energy and some of the geometrical parameters. The absolute value of the stacking energy correlates negatively with the distance (Fig. 5) and positively with the

shift, whereas it appears to be relatively independent of the tilt and the phase. This means that the most favorable stacking is obtained when the rings lie close to each other and are somewhat shifted. Indeed, perfectly stacked rings with zero shift are less stable than parallel-displaced rings. The xylenes have higher shifts and lower distances than the dichlorobenzenes, thus explaining the systematically stronger stacking energy of the xylenes. The benzene pair is an outlier and does not follow this trend.

3.2 MIL-47 packed with four xylenes: decomposition of the adsorption energy

The stacking of xylenes is a favorable interaction in the gas phase of the order of -31.7 kJ/mol. Since the walls of the MIL-47 pores contain aromatic rings in the terephthalic linkers, it is expected that adsorbed xylenes are stabilized by an additional stacking energy: the interaction between the adsorbed xylenes and the framework, that is, the so-called host–guest interactions. We have investigated the geometrical characteristics and adsorption energy when MIL-47 is loaded with a xylene pair in each of its pores, which amounts to a total of four xylenes (two pairs) per unit cell. The adsorption energy is calculated as the difference in energy between the framework wherein two

Table 1 The geometrical parameters (shift s, distance d, tilt θ, and phase φ) and stacking energy (Eq. 1) calculated for the optimized structure with lowest energy and calculated as a thermal average

	Lowest energy geometry					300 K	Thermal average 300 K				
	Shift (Å)	Distance (Å)	Tilt (°)	Phase (°)	ΔE_{stack}^{vac} (kJ/mol)	$p(E_1)$	⟨Shift⟩ (Å)	⟨Distance⟩ (Å)	⟨Tilt⟩ (°)	⟨Phase⟩ (°)	⟨ΔE_{stack}^{vac}⟩ (kJ/mol)
Bz–Bz	1.66	3.22	5.5	9.0	−19.7	1.0	1.66	3.22	5.5	9.0	−19.7
pX–pX	0.8	3.27	3.3	38.5	−31.1	0.3	0.6	3.31	4.0	80.3	−28.5
oX–oX	1.3	3.25	2.6	41.9	−32.6	0.8	1.1	3.30	3.3	47.6	−30.3
mX–mX	1.5	3.22	4.7	104.9	−33.0	0.4	1.2	3.28	5.3	75.1	−30.6
pX–oX	1.3	3.34	4.2	102.5	−34.5	0.3	1.3	3.30	3.6	162.7	−32.7
pX–mX	1.4	3.20	8.9	−15.8	−36.3	0.5	1.3	3.23	7.5	29.0	−33.8
oX–mX	1.5	3.28	1.0	−26.9	−37.1	0.5	1.3	3.27	2.4	−25.3	−34.4
Average	*1.3*	*3.26*	*4.1*	*40.8*	*−34.1*	*0.4*	*1.1*	*3.28*	*4.4*	*61.6*	*−31.7*
pCl–pCl	1.1	3.17	4.1	59.4	−28.0	0.3	0.5	3.30	3.2	80.5	−24.1
oCl–oCl	0.9	3.27	2.9	124.6	−27.8	0.2	0.6	3.33	2.4	140.5	−25.2
mCl–mCl	0.4	3.40	9.6	64.0	−24.8	0.1	0.3	3.40	5.0	85.8	−21.6
pCl–oCl	0.9	3.28	1.9	152.5	−25.1	0.1	0.5	3.36	4.9	168.8	−22.5
pCl–mCl	0.9	3.23	5.9	91.7	−28.3	0.2	0.8	3.29	4.2	84.5	−25.3
oCl–mCl	1.0	3.24	2.5	−149.5	−29.9	0.3	0.8	3.29	2.3	−123.1	−27.0
Average	*0.9*	*3.27*	*4.5*	*57.1*	*−27.3*	*0.2*	*0.6*	*3.33*	*3.7*	*72.8*	*−24.3*

The probability $p(E_1)$ to find the structure in the lowest energy state at 300 K is also listed. Averages in the table are taken over the six xylene pairs and over the six dichlorobenzene pairs

pairs (P_{12}, P_{34}) are adsorbed, the empty framework (F), and the individual xylene molecules (X_1, X_2, X_3, X_4),

$$\Delta E_{ads}(P_{12}, P_{34}) = E(F, P_{12}, P_{34}) - E(F) - E^{vac}(X_1) \\ - E^{vac}(X_2) - E^{vac}(X_3) - E^{vac}(X_4) \quad (4)$$

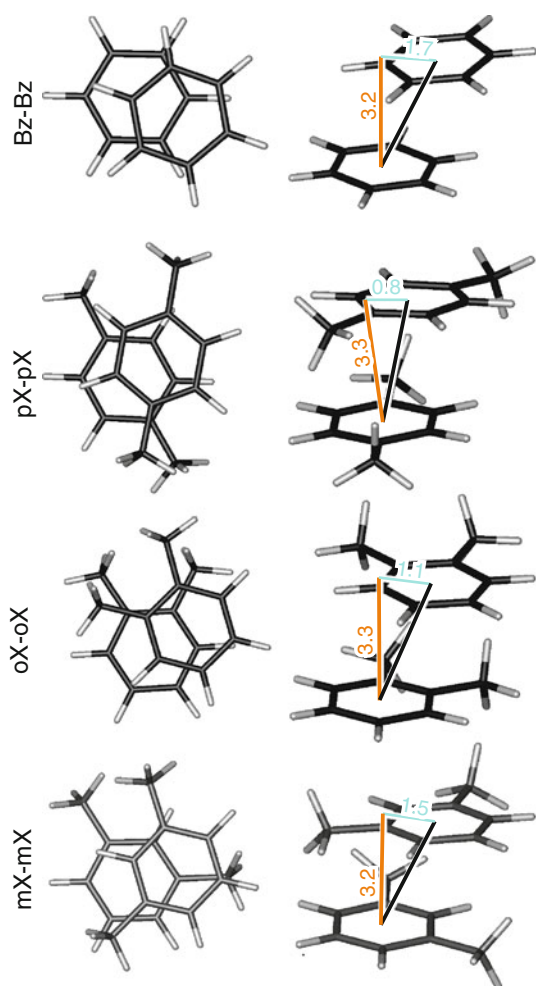Both guest–guest and guest–host interactions contribute to this adsorption energy.

In order to find the most favorable configurations of xylene pairs in the framework, an extensive set of initial structures is generated in a similar fashion as in the gas phase analysis in Sect 2.1. Each unit cell contains two pores, and each pore is filled with a xylene pair. As in the gas phase, the list of pair geometries is generated systematically by varying the distance d between 2.8 and 4.0 Å in steps of 0.2 Å and by varying the phase φ in steps of 30°. This gives 231 initial pair geometries, as shown in Fig. 3. However, the confinement in the pore prevents some of the proposed pairs to be adsorbed (these orientations are given a red background in Fig. 3), leaving 161 plausible initial pair geometries. We adopt now the following procedure, as depicted in Fig. 6: for each of the plausible pair geometries, a duplicate is placed in the center of the first pore and another in the center of the second pore. This procedure results in 161 initial structures for fully loaded MIL-47.

An extra degree of freedom in the adsorbed state, compared to the gas phase, is the relative orientation of a pair as a whole with respect to the framework. Whereas rotating a pair or applying symmetry operations does not affect the energy in vacuum, this symmetry is broken when a pair is brought in the pores. Our 161 initial structures only represent 23 possible pair orientations. Unfortunately, a full sampling of this orientational degree of freedom is computationally not feasible. Nevertheless, we have added 15 orientations to improve the sampling, mainly for the mixed pairs which have lower symmetry than the pure pairs. In total, 266 initial structures for the fully loaded MIL-47 are created and optimized.

The geometry of each initial structure for the fully loaded state is optimized. Figure 7 shows the resulting geometries of the adsorbed pure pairs, and the mixed pairs are given in Figures 6–8 of the Supp. Info. For a given pore filling, the geometries are ordered according to increasing energy and the probability distribution is calculated (Eq. 2). Since the Boltzmann distribution is peaked (Supp. Info. Fig. 2), only the dominant geometry with the lowest energy is considered in the remainder of this section.
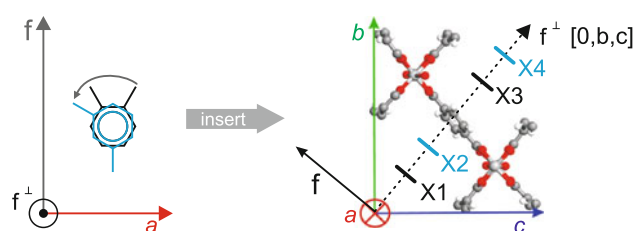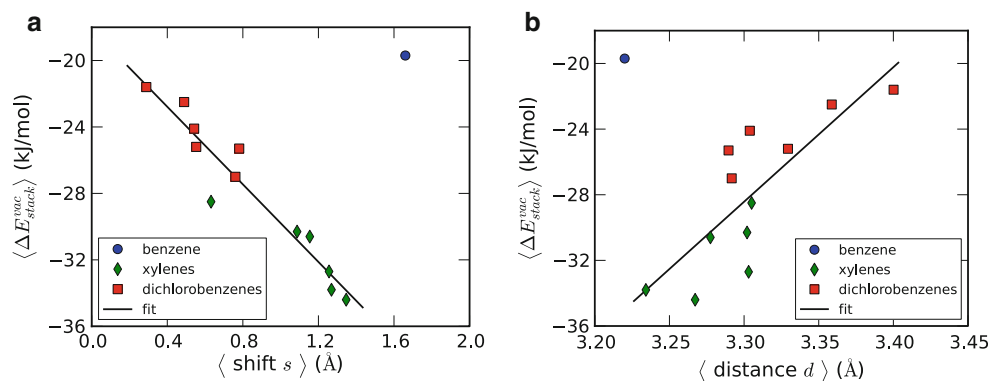
Comparison of the geometrical parameters of the adsorbed pairs (Table 2) with the pairs in vacuum (Table 1) shows that the distance is similar to the values for the adsorbed pairs in vacuum and that the shift has increased. Whereas the tilt takes values up to 34.1° in the adsorbed state, it remains close to zero in vacuum. In gas phase, this could be a consequence of our selection of initial structures where the tilt has been put to zero
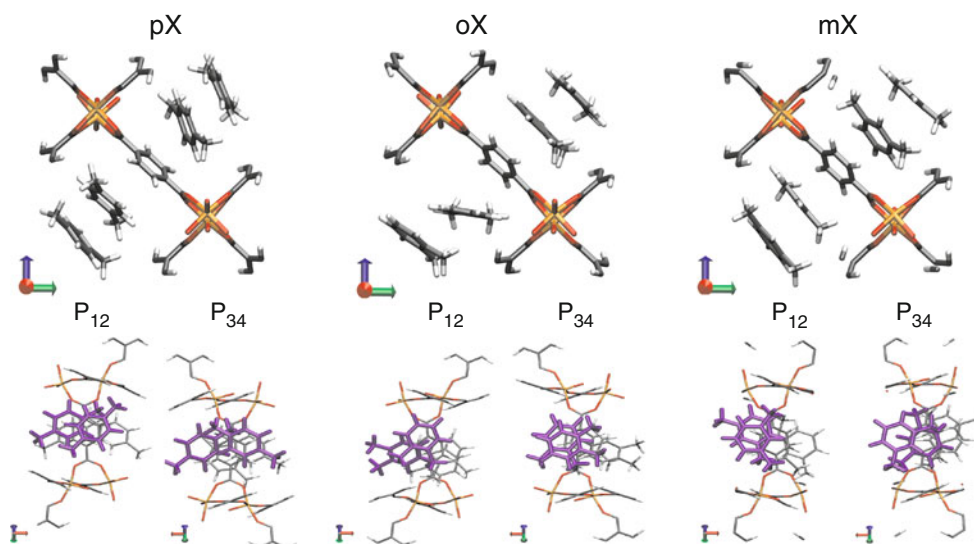
Fig. 6 The initial geometries of the fully loaded framework are created by inserting the xylene pairs of Fig. 3 into the MIL-47 pores. The vectors f and $f^{\perp}$ denote the diagonals in the (b, c) plane, orthogonal to the a direction. The pairs are inserted at the origin and translated over the vector $0.5a$. Subsequently, one pair is translated over the vector $0.25f^{\perp}$ and the other over the vector $0.75f^{\perp}$

Fig. 4 Some stacked pairs in the gas phase viewed along the z_1 axis and sideways: benzene pair and pure pX, oX, and mX xylene pairs. The *orange* and *blue line* indicate the distance d and shift s parameters, respectively

The selectivity of xylene isomers in MIL-47 has earlier been attributed to geometrical packing effects [8, 9]. From X-ray data at high loadings [8, 9], it was suggested that molecules are adsorbed by pairs, with their aromatic rings facing each other. The occurrence of certain geometrical effects for single-component adsorption obtained by Rietveld refinement is as follows [8].

1. pX: The methyl groups within a stacked para-xylene pair are perfectly staggered.
2. oX: Structure refinement of ortho-xylene pairs reveals that the stacking of these isomers is analogous to that of para-xylene, but ring alignment is slightly less effective: the rings are shifted with respect to each other.
3. mX: Within pairs of meta-xylene, a steric interaction arises between an aromatic ring of one molecule and a methyl group of a molecule in the neighboring unit cell in the a direction. This interaction causes a tilt and a rotation of the aromatic molecules, preventing the optimal stacking of the rings.

In the three cases, the methyl groups dictate the spatial arrangement of the pairs. However, these experimental geometries differ from our most stable optimized structures (visualized in Fig. 7 and Figures 6–8 of Supp. Info.): the rings of the energetically most stable structures are often

systematically. When the pair is brought into the pore, the xylenes have to reorient themselves to attain optimal stacking with the terephthalic framework linkers, thus causing the large rotation.

Fig. 5 The stacking energy of the pairs becomes stronger with increasing shift s and decreasing distance d. The benzene pair is an outlier; the linear fits are based on the thermal average values at 300 K of the xylene and dichlorobenzene pairs

Fig. 7 The most stable geometry of the pure pX, oX, and mX pairs adsorbed in MIL-47. *Top* one unit cell viewed along the one-dimensional channels, in the *a* direction (*red arrow*), loaded with four xylenes. *Bottom* for each adsorbed state, the geometry of the P_{12} and P_{34} pairs is highlighted in purple in a view along the vector $f^{\perp}$, as defined in Fig. 6, for P_{12} and in the opposite sense (vector $-f^{\perp}$) for P_{34}

Table 2 Geometrical parameters of individual xylene pairs P_{12} and P_{34} in their adsorbed state

	Pair P_{12} in first pore				Pair P_{34} in second pore			
	Shift (Å)	Distance (Å)	Tilt (°)	Phase (°)	Shift (Å)	Distance (Å)	Tilt (°)	Phase (°)
pX–pX	3.8	3.17	23.0	246.5	2.1	3.26	24.8	21.1
oX–oX	1.2	3.20	6.3	109.2	3.2	3.03	26.3	69.1
mX–mX	2.8	3.11	23.3	154.3	1.3	3.26	6.5	140.3
pX–oX	1.3	3.27	5.1	216.3	1.8	3.14	5.8	219.9
pX–mX	1.8	3.57	33.3	3.0	1.7	3.24	3.1	−23.0
oX–mX	2.9	3.33	34.1	56.7	1.6	3.21	9.2	49.6
Average	*2.3*	*3.3*	*20.9*	*131.0*	*2.0*	*3.2*	*12.6*	*79.5*

not parallel (tilt θ) and are shifted (shift s). Such a more random ordering was also observed by Castillo et al. [20] in GCMC simulations of a fully packed $4 \times 2 \times 2$ unit cell. Their unordered embedding of the ortho-xylenes in the pores resembles the configuration of our oX pair P_{34} [20]. They only found ordering for the pX pairs, in which all CH$_3$ groups between neighboring cells have the same orientation, resembling the geometry of our pX pair P_{12}.

3.3 Decomposition of adsorption energy in MIL-47

The adsorption energy is influenced by three effects: framework deformation, interaction of xylenes with the pore walls, and stacking of xylenes. The adsorption energy is thus decomposed into three terms

$$\Delta E_{\text{ads}} = E_{\text{deform}} + E_{\text{inter}} + E_{\text{stack}} \tag{5}$$

The physical interpretation of the terms is visualized in Fig. 8, and the calculated values are reported in Table 3.
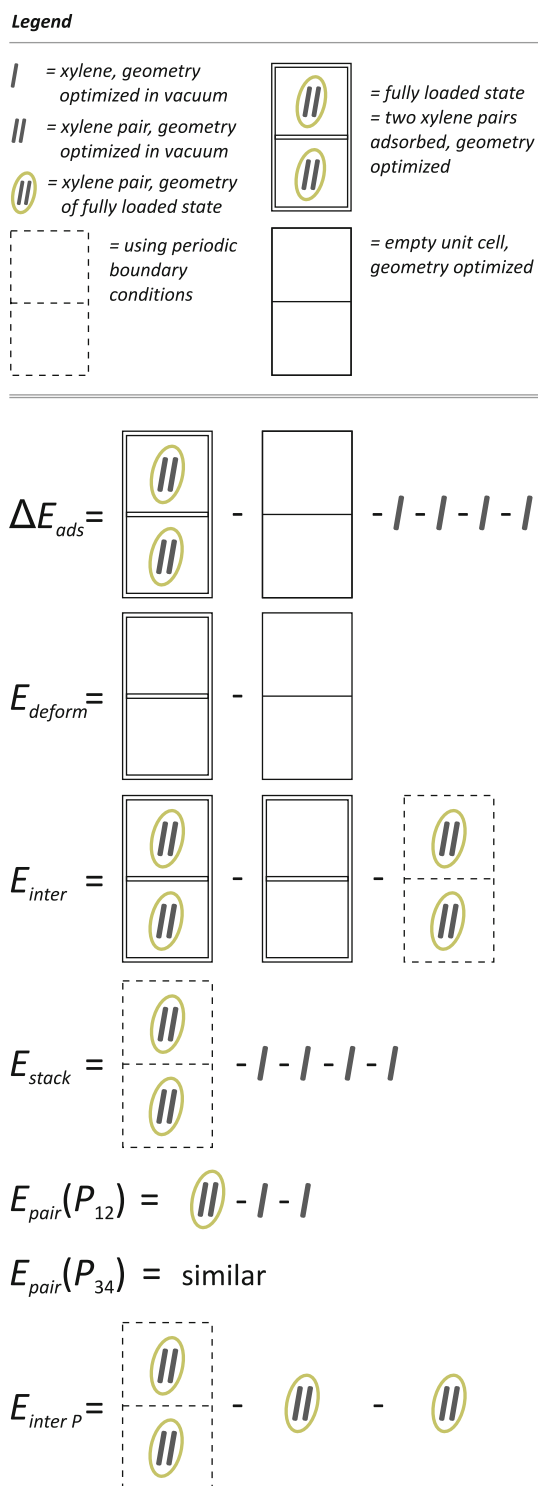
A first contribution is the framework deformation. In order to accommodate the xylene pairs in the pores, the structure needs to relax and the linkers may need to reorient. This effect is quantified by the deformation energy E_{deform}, which is defined as the difference in energy between the empty framework with its geometry as in the fully adsorbed state (F, stat) and the empty framework with its geometry relaxed (F),

$$E_{\text{deform}} = E^{\text{stat}}(F) - E(F) \tag{6}$$

The framework deformation due to the loading requires energy ($E_{\text{deform}} > 0$).

A second contribution is the host–guest interactions. The xylenes are physisorbed in the pores due to interactions with the framework. The interaction energy E_{inter} is defined as the energy difference of the fully loaded framework (F, P_{12}, P_{34}) with respect to the energy of the empty host (F, stat) and the energy of the xylenes pairs (P_{12}, P_{34}, stat).

Legend

I = xylene, geometry optimized in vacuum

II = xylene pair, geometry optimized in vacuum

II = xylene pair, geometry of fully loaded state

= using periodic boundary conditions

= fully loaded state = two xylene pairs adsorbed, geometry optimized

= empty unit cell, geometry optimized

$\Delta E_{ads} =$

$E_{deform} =$

$E_{inter} =$

$E_{stack} =$

$E_{pair}(P_{12}) =$

$E_{pair}(P_{34}) =$ similar

$E_{inter\,P} =$

Fig. 8 Visualization of the decomposition of the adsorption energy (Eq. 5): the deformation energy (Eq. 6), the xylene–framework interaction (Eq. 7), and the stacking energy (Eq. 10) are calculated by deleting the xylenes or the framework from the fully loaded framework, and performing static calculations. The stacking energy is further decomposed in pair energies (Eq. 8) and the inter-pair energy (Eq. 9)

$$E_{inter} = E(F, P_{12}, P_{34}) - E^{stat}(F) - E^{stat}(P_{12}, P_{34}) \qquad (7)$$

The latter two static calculations are simple single-point energy computations using the same geometry as in the fully loaded host (no geometry optimization is performed) from which the xylenes or the framework are removed (Fig. 8). The interaction of the xylenes with the pore walls, in this case mainly the terephthalic linkers, is attractive ($E_{inter} < 0$).

The third contribution in Eq. (5) is the interaction E_{stack} between the xylene molecules. As the xylenes appear in pairs in the pores, a large part of these xylene interactions per unit cell is the stacking energy of the first pair E_{pair} (P_{12}) and the stacking energy of the second pair E_{pair} (P_{34}). Due to the interaction with the host, the xylene pairs have different geometries than in vacuum. Instead of using Eq. (1), these pair stacking energies should be calculated by comparing the energy of an isolated pair in vacuum with the energies of two individual xylenes in vacuum. For instance, the geometry of the isolated pair P_{12} is obtained by removing the framework and pair P_{34} from the optimized fully loaded state. The static energy of this P_{12} geometry is then calculated with a single-point computation in a large box (vacuum, P_{12}, stat),

$$E_{pair}(P_{12}) = E^{stat,vac}(P_{12}) - E^{vac}(X_1) - E^{vac}(X_2) \qquad (8)$$

and similarly for pair P_{34}. The pair stacking energy is schematically visualized in Fig. 8.

The remainder of the adsorption energy represents interactions between xylene pairs due to the periodicity of the material and is labeled as the inter-pair interaction E_{interP}. A xylene pair interacts with other adsorbed xylene pairs in its own channel as well as with xylene pairs in adjacent channels. The interaction is calculated from the static energy of the pairs in the fully loaded geometry, where the framework has been removed, with the periodicity set to the framework lattice parameters (P_{12}, P_{34}, stat). This energy is compared with the static energy of the individual pairs, still in the same geometry, using a large box (vacuum, P_{12}, stat and vacuum, P_{34}, stat).

$$E_{interP} = E^{stat}(P_{12}, P_{34}) - E^{stat,vac}(P_{12}) - E^{stat,vac}(P_{34})$$
$$(9)$$

This procedure measures the interaction between the two pairs and the interaction with the periodic images of the pairs. Similar to the stacking energy of two molecules, the inter-pair interaction is favorable for the adsorption ($E_{interP} < 0$). The total stacking energy in Eq. (5), which is also a negative contribution, can now be calculated as the sum of the pair stacking energies and the inter-pair stacking:

Table 3 Energy contributions to the adsorption energy of the fully loaded framework: deformation energy of the framework (E_{deform}), interaction energy between xylenes and framework (E_{inter}), and xylene stacking energy (E_{stack})

	ΔE_{ads}			E_{stack}			ΔE_{ads}	$\Delta E_{ads}/4$
	E_{deform}	E_{inter}	E_{stack}	E_{pair} (P_{12})	E_{pair} (P_{34})	E_{interP}		
MIL-47 + 4pX	19.3	−120.8	−131.2	−29.1	−18.4	−83.7	−232.7	−58.2
MIL-47 + 4oX	29.3	−120.1	−137.4	−26.9	−34.1	−76.5	−228.3	−57.1
MIL-47 + 4mX	18.8	−138.3	−109.2	−31.8	−37.2	−40.3	−228.8	−57.2
MIL-47 + 2pX–oX	15.6	−134.4	−103.9	−30.9	−35.9	−37.2	−222.8	−55.7
MIL-47 + 2pX–mX	8.0	−147.0	−116.0	−28.8	−22.3	−65.0	−255.0	−63.8
MIL-47 + 2oX–mX	5.9	−141.9	−95.0	−27.6	−25.2	−42.2	−231.0	−57.7
Average	16.2	−133.8	−115.5	−29.2	−28.9	−57.5	−233.1	−58.3

The stacking energy consists of the stacking energies of the individual pairs and the inter-pair stacking energy. The adsorption energy per xylene is obtained by division by four. All energies in kJ/mol

$$E_{stack} = E_{pair}(P_{12}) + E_{pair}(P_{34}) + E_{interP} \qquad (10)$$

The predicted total adsorption energies are on average −233.1 kJ/mol per unit cell (Table 3), which amounts to −58.3 kJ/mol per adsorbed xylene molecule. On average, the host–xylene interaction E_{inter} and the xylene stacking energy E_{stack} contribute equally. But in individual cases, we notice some significant deviations: the total stacking energy can vary by more than 40 kJ/mol. Nevertheless, this effect is mostly compensated by the interaction energy between the xylenes and the walls of the host. A large stacking energy of the xylenes is accompanied systematically by a higher repulsive deformation energy of the framework. This feature could be understood by assuming that some framework relaxation is required to accommodate the xylene pair in its most favorable stacked conformation.

Within the category of pure pairs, the xylene–framework interaction energy is by far the strongest for the adsorption of pure mX pairs (−138.3 kJ/mol). The trend to favor mX is maintained when using mixed pairs, since the adsorption of mixed pairs oX–mX or pX–mX shows by far the largest interaction energies with the host. However, these favorable interactions are partially cancelled out by the lower stacking energies. Note also that more favorable energies for pure pairs not systematically lead to more favorable energies in the mixed pairs. For instance, mixing with the xylene isomer with the strongest stacking energy (oX) does not result in the strongest stacking energies for the mixed pairs (oX–mX, oX–pX). From Table 3, we conclude that the data for pure pairs are insufficient to predict adsorption energetics for mixed pairs.

The decomposition of the stacking energy in Table 3 shows that the pair stacking energies of the adsorbed pairs are less favorable than those of the pairs in vacuum (average −31.7 kJ/mol). Nevertheless, the pair stacking attains an average stacking efficiency of (−29.2 − 28.9)/2 = −29.0 kJ/mol. The inter-pair stacking energy can be very large, up to −83.7 kJ/mol for pX. The variation in the inter-pair stacking is explained by the organization of the xylenes in the pores, which may be derived from the geometrical parameters as follows. It is clear from Fig. 6 that X_1 and X_2 are nearest neighbors in the channel, and X_3 and X_4 are nearest neighbors in the adjacent channel. The interaction of a xylene with its nearest neighbors is included in the pair stacking energies E_{pair} (P_{12}) and E_{pair} (P_{34}). The interaction of xylenes with their next nearest neighbors is then of course included in the E_{interP}. According to our geometry versus energy analysis in vacuum (Fig. 5), the strength of the xylene–xylene interaction is mainly determined by the distance between the two molecules. To see the effect of the distance on the inter-pair energy, we determined the distance from the xylenes to their second nearest neighbor, which should be the dominant contribution. This distance is calculated as the root of $s^2 + d^2$ (s and d as defined in Fig. 2), which equals the distance between the centers of their rings. For pX, the second neighbors are separated by 4.96 and 5.77 Å, and these relatively short separations result in the strong inter-pair stacking energy of −83.7 kJ/mol. In contrast, the second neighbors for mX are separated by 5.75 and 7.40 Å, resulting in a much weaker inter-pair energy of −40.3 kJ/mol.

The typical stacking energy in vacuum, about −31.7 kJ/mol (Table 1), may be used as a 'unit for energy' to compare the importance of the energy contributions. The interaction energy of two pairs with the framework is worth over four units, the stacking of the pairs is worth one unit each, the inter-pair stacking is worth two units, and the deformation diminishes the total by half a unit. This brings the adsorption energy to nearly eight vacuum stacking energy equivalents (−233.1 kJ/mol). The attractive stacking between xylene molecules is here of the same importance as the attractive interaction energy between xylenes and framework.

Summarizing, the pure pairs deform the framework more (larger positive E_{deform}) and interact more weakly

with the framework (weaker E_{inter}) than the mixed pairs. However, the pure xylene pairs stack more efficiently in the pores (stronger E_{stack}). Overall, the values of adsorption energy for the various xylene pairs all have the same order of magnitude and appear not to explain the different adsorption selectivity of the pX, oX, and mX isomers. If the pure adsorption isotherms were to be solely determined by the strength of the adsorption energy, one would need a strong adsorption energy for pX, followed by oX, and a considerably weaker adsorption energy for mX. Since this is not the case, our results indicate that the selective adsorption behavior cannot be explained purely energetically. This means that temperature and entropy are expected to play a determining role for the selectivity.

The entropy arises from the many possible configurations the xylenes can take when adsorbed in the pores. In general, the more configurations the xylenes can take within the pores, the higher the entropy, and the more favorable the adsorption. A first contribution to the entropy is the relative orientation of the molecules in a xylene pair. The presence of the methyl groups can here reduce the number of configurational states. The fewer states are prohibited (because of overlapping methyl groups), the more states are available, and the more entropy is available. A second contribution to the entropy is the positioning of the pair in the channels. Likewise, the pair may take a number of different orientations and positions inside the channels. Bulkier pairs show a more limited number of available configurations, leading to a lower entropy. A third entropic contribution arises in the process of multicomponent adsorption, referred to as mixing entropy. Many ways exist to distribute the xylenes of each kind over the pores. The information about entropy is lacking in adsorption energy calculations, but could be obtained by a vibrational analysis [47, 48], Monte Carlo or Molecular Dynamics simulations. GCMC calculations, as those by Castillo et al. [20], include energetic and entropic effects and agree with experimental single-component isotherms. Our study now shows that the energetics of the pure and mixed xylene adsorption at high loadings are not alone responsible for the selectivities between isomers, such that the separation is also entropically driven.

4 Conclusions

The molecular packing effects of xylene isomers inside the confining environment of the MIL-47 pore system have been studied by quantumchemical calculations. The guest–guest interactions are first quantified in the gas phase. Xylenes show a high stacking energy in vacuum, such that xylenes are expected to stack efficiently with the rings of the MIL-47 linkers. When the xylenes are inserted in the MIL-47 pores, not only guest–guest interactions contribute to the adsorption energy, but also host–guest interactions. The adsorption energy for high loadings of para-, ortho-, and meta-xylene has thus been decomposed in three contributions: the deformation energy of the framework, the framework–xylene interaction, and the stacking energy. The stacking energy has been found to be equally important as the framework–xylene interaction, hence confirming the hypothesis that π–π stacking is responsible for the adsorption. The average stacking energy of xylene pairs in vacuum can be used as a unit for the interactions. The adsorption energy in the fully loaded state amounts to nearly two vacuum stacking equivalents per adsorbed xylene, which explains the efficient adsorption at room temperature.

The energetics could not explain the experimentally observed separation of xylene isomers with a preferential adsorption for ortho-xylene and para-xylene, since all adsorption energies lie in the same range. Therefore, entropic effects are likely the main driving force for the adsorption selectivity. This has two implications. First, sampling of configurational space should be adequately performed to assess the entropic effects, which can only be obtained with molecular dynamics or Monte Carlo simulations. Second, since the accuracy of the energetics is of subordinary importance to the sampling, it is expected that reasonable results can be obtained with classical force fields. Whereas force fields are less accurate than an ab initio treatment, they allow considerably longer sampling times because of the reduced computational cost.

References

1. Férey G (2008) Hybrid porous solids: past, present, future. Chem Soc Rev 37:191–214
2. Long JR, Yaghi OM (2009) The pervasive chemistry of metal-organic frameworks. Chem Soc Rev 38:1213–1214
3. Perry JJ, Perman JA, Zaworotko MJ (2009) Design and synthesis of metal-organic frameworks using metal-organic polyhedra as supermolecular building blocks. Chem Soc Rev 38:1400–1417
4. Eddaoudi M, Kim J, Rosi N, Vodak D, Wachter J, O'Keeffe M, Yaghi OM (2002) Systematic design of pore size and functionality in isoreticular MOFs and their application in methane storage. Science 295:469–472
5. Férey G, Serre C, Devic T, Maurin G, Jobic H, Llewellyn PL, De Weireld G, Vimont A, Daturi M, Chang JS (2011) Why

hybrid porous solids capture greenhouse gases? Chem Soc Rev 40:550–562

6. Meek ST, Greathouse JA, Allendorf MD (2011) Metal-organic frameworks: a rapidly growing class of versatile nanoporous materials. Adv Mater 23:249–267

7. Tranchemontagne DJ, Mendoza-Cortes JL, O'Keeffe M, Yaghi OM (2009) Secondary building units, nets and bonding in the chemistry of metal-organic frameworks. Chem Soc Rev 38:1257–1283

8. Alaerts L, Kirschhock CEA, Maes M, van der Veen MA, Finsy V, Depla A, Martens JA, Baron GV, Jacobs PA, Denayer JEM, De Vos DE (2007) Selective adsorption and separation of xylene isomers and ethylbenzene with the microporous vanadium(IV) terephthalate MIL-47. Angew Chem Int Edit 46:4293–4297

9. Finsy V, Verelst H, Alaerts L, De Vos D, Jacobs PA, Baron GV, Denayer JFM (2008) Pore-filling-dependent selectivity effects in the vapor-phase separation of xylene isomers on the metal-organic framework MIL-47. J Am Chem Soc 130:7110–7118

10. Vermoortele F, Maes M, Moghadam PZ, Lennox MJ, Ragon F, Boulhout M, Biswas S, Laurier KGM, Beurroies I, Denoyel R, Roeffaers M, Stock N, Düren T, Serre C, De Vos DE (2011) p-xylene-selective metal–organic frameworks: a case of topology-directed selectivity. J Am Chem Soc 133:18526–18529

11. Fritz Ullmann's encyclopedia of industrial chemistry, 6th edn. In: Electronic release, 2000

12. Barthelet K, Marrot J, Riou D, Férey G (2002) A breathing hybrid organic-inorganic solid with very large pores and high magnetic characteristics. Angew Chem Int Edit 41:281

13. Grimme S (2006) Semiempirical GGA-type density functional constructed with a long-range dispersion correction. J Comput Chem 27:1787–1799

14. Grimme S, Antony J, Schwabe T, Muck-Lichtenfeld C (2007) Density functional theory with dispersion corrections for supramolecular structures, aggregates, and complexes of (bio)organic molecules. Org Biomol Chem 5:741–758

15. Schwabe T, Grimme S (2008) Theoretical thermodynamics for large molecules: walking the thin line between accuracy and computational cost. Acc Chem Res 41:569–579

16. Liu B, Smit B (2009) Comparative molecular simulation study of CO_2/N_2 and CH_4/N_2 separation in zeolites and metal—organic frameworks. Langmuir 25:5918–5926

17. Ramsahye NA, Maurin G, Bourrelly S, Llewellyn PL, Devic T, Serre C, Loiseau T, Férey G (2007) Adsorption of CO_2 in metal organic frameworks of different metal centres: grand Canonical Monte Carlo simulations compared to experiments. Adsorpt J Int Adsorpt Soc 13:461–467

18. Rosenbach N, Jobic H, Ghoufi A, Salles F, Maurin G, Bourrelly S, Llewellyn PL, Devic T, Serre C, Férey G (2008) Quasi-elastic neutron scattering and molecular dynamics study of methane diffusion in metal organic frameworks MIL-47(V) and MIL-53(Cr). Angew Chem Int Edit 47:6611–6615

19. Salles F, Jobic H, Maurin G, Koza MM, Llewellyn PL, Devic T, Serre C, Férey G (2008) Experimental evidence supported by simulations of a very high H-2 diffusion in metal organic framework materials. Phys Rev Lett 100(24):245901

20. Castillo JM, Vlugt TJH, Calero S (2009) Molecular simulation study on the separation of xylene isomers in MIL-47 metal—organic frameworks. J Phys Chem C 113:20869–20874

21. Wang S, Yang Q, Zhong C (2008) Adsorption and separation of binary mixtures in a metal-organic framework Cu-BTC: a computational study. Sep Purif Technol 60:30–35

22. Hamon L, Llewellyn PL, Devic T, Ghoufi A, Clet G, Guillerm V, Pirngruber GD, Maurin G, Serre C, Driver G, Beek WV, Jolimaître E, Vimont A, Daturi M, Férey GR (2009) Co-adsorption and separation of CO_2–CH_4 mixtures in the highly flexible MIL-53(Cr) MOF. J Am Chem Soc 131:17490–17499

23. Gallo M, Glossman-Mitnik D (2009) Fuel gas storage and separations by Metal—organic frameworks: simulated adsorption isotherms for H_2 and CH_4 and their equimolar mixture. J Phys Chem C 113:6634–6642

24. Pan L, Olson DH, Ciemnolonski LR, Heddy R, Li J (2006) Separation of hydrocarbons with a microporous metal-organic framework. Angew Chem Int Edit 45:616–619

25. Vanduyfhuys L, Verstraelen T, Vandichel M, Waroquier M, Van Speybroeck V (2012) Ab initio parametrized force field of the metal-organic framework MIL-53(Al) for use in molecular simulations including lattice dynamics. J Chem Theory Comput (submitted)

26. Sinnokrot MO, Sherrill CD (2003) Unexpected substituent effects in face-to-face π-stacking interactions. J Phys Chem A 107:8377–8379

27. Sinnokrot MO, Sherrill CD (2004) Highly accurate coupled cluster potential energy curves for the benzene dimer: sandwich, T-shaped, and parallel-displaced configurations. J Phys Chem A 108:10200–10207

28. Sinnokrot MO, Sherrill CD (2004) Substituent effects in π–π interactions: sandwich and T-shaped configurations. J Am Chem Soc 126:7690–7697

29. Alaerts L, Maes M, Jacobs PA, Denayer JFM, De Vos DE (2008) Activation of the metal-organic framework MIL-47 for selective adsorption of xylenes and other difunctionalized aromatics. Phys Chem Chem Phys 10:2979–2985

30. Cremer D, Pople JA (1975) General definition of ring puckering coordinates. J Am Chem Soc 97:1354–1358

31. Car R, Parrinello M (1985) Unified approach for molecular dynamics and density-functional theory. Phys Rev Lett 55:2471–2474

32. Becke AD (1988) Density-functional exchange-energy approximation with correct asymptotic behavior. Phys Rev A 38:3098

33. Vanderbilt D (1990) Soft self-consistent pseudopotentials in a generalized eigenvalue formalism. Phys Rev B 41:7892

34. Verstraelen T, Van Speybroeck V, Waroquier M (2008) ZEO-BUILDER: a GUI toolkit for the construction of complex molecular structures on the nanoscale with building blocks. J Chem Inf Model 48:1530–1541

35. Gu J, Wang J, Leszczynski J, Xie Y, Schaefer HF (2008) Chem Phys Lett 459:164

36. McGaughey GB, Gagne M, Rappe AK (1998) J Biol Chem 273:15458

37. Morgado C, Vincent MA, Hillier IH, Shan X (2007) Phys Chem Chem Phys 9:448

38. Pavone M, Rega N, Barone V (2008) Chem Phys Lett 452:333

39. Piacenza M, Grimme S (2004) J Comput Chem 25:83

40. Podeszwa R, Bukowski R, Szalewicz K (2006) J Phys Chem A 110:10345

41. Waller MP, Robertazzi A, Platts JA, Hibbs DE, Williams PA (2006) J Comput Chem 27:491

42. Zhao Y, Truhlar DG (2005) Phys Chem Chem Phys 7:2701

43. Zhao Y, Truhlar DG (2006) J Chem Theory Comput 2:1009

44. Lee EC, Hong BH, Lee JY, Kim JC, Kim D, Kim Y, Tarakeshwar P, Kim KS (2005) Substituent effects on the edge-to-face aromatic interactions. J Am Chem Soc 127:4530–4537

45. Raju RK, Bloom JWG, An Y, Wheeler SE (2011) Substituent effects on non-covalent interactions with aromatic rings: insights from computational chemistry. ChemPhysChem 12:3116–3130

46. Hohenstein EG, Duan JN, Sherrill CD (2011) Origin of the surprising enhancement of electrostatic energies by electron-donating substituents in substituted sandwich benzene dimers. J Am Chem Soc 133:13244–13247

47. De Moor BA, Ghysels A, Reyniers M-F, Van Speybroeck V, Waroquier M, Marin GB (2011) Normal mode analysis in zeolites: toward an efficient calculation of adsorption entropies. J Chem Theory Comput 7:1090–1101

48. Van der Mynsbrugge J, Hemelsoet K, Vandichel M, Waroquier M, Van Speybroeck V (2012) An efficient approach for the computational study of alcohol and nitrile adsorption in H-ZSM-5. J Phys Chem C 116:5499–5508